TEARING MODE INSTABILITY IN A FIELD-REVERSED ION LAYER

Han S. Uhm
Naval Surface Weapons Center
White Oak, Silver Spring, Maryland 20910

Ronald C. Davidson
Plasma Fusion Center
Massachusetts Institute of Technology
Cambridge, Massachusetts 02139

PFC/JA-79-2

Submitted to Physics of Fluids,
February 1979

TEARING MODE INSTABILITY IN A FIELD-REVERSED ION LAYER

Han S. Uhm
Naval Surface Weapons Center
White Oak, Silver Spring, Maryland 20910

Ronald C. Davidson
Plasma Fusion Center
Massachusetts Institute of Technology
Cambridge, Massachusetts 02139

Tearing mode stability properties are investigated for azimuthally symmetric perturbations about an intense proton layer (P-layer) immersed in a background plasma. The analysis is carried out within the framework of a hybrid-kinetic model. It is assumed that the layer is thin, with radial thickness (2a) much smaller than the mean radius (R_0). Tearing mode stability properties are investigated for the choice of ion layer distribution function in which all ions have the same perpendicular energy in a frame rotating with angular velocity ω_θ and a step-function distribution in axial velocity v_z. Moreover, the stability analysis is carried out for low-frequency perturbations with $|\omega| \lesssim \omega_{ci}$. The dispersion relation is derived including the important dielectric influence of the background plasma and the background layer electrons. It is shown that an axial velocity spread stabilizes perturbations with sufficiently short axial wavelength. Moreover, the tearing mode growth rate is significantly reduced whenever $n_p/n_b \gg 1$, where n_p is the background plasma density and n_b is the density of layer ions.

I. INTRODUCTION

In recent years, there has been a renewed interest in field-reversed layers and rings as magnetic confinement configurations for fusion plasmas.[1-5] Such field-reversed configurations are likely subject to various macro- and microinstabilities.[5-10] For example, the tearing-mode stability properties[11] of a field-reversed E-layer (electron layer) has been investigated by Marx[5] for azimuthally symmetric perturbations in the absence of a background plasma. A more general analysis is required to investigate stability properties for an intense field-reversed ion layer characterized by $\nu \gtrsim 1$ and $n_p \gtrsim n_b$. Here $\nu = N_b e^2/m_i c^2$ is Budker's parameter for the layer ions, $N_b = 2\pi\int_0^{R_c} dr\, r\, n_b^0(r)$ is the number of ions per unit axial length, and n_p and n_b are the plasma density and density of layer ions, respectively. The present paper examines the tearing mode stability properties of an intense ion layer immersed in a background plasma. It is assumed that the perturbations are azimuthally symmetric ($\partial/\partial\theta = 0$), and the analysis is restricted to low frequency perturbations with $|\omega| \lesssim \hat{\omega}_{ci} = eB_0/m_i c$. Here, ω is the complex eigenfrequency and $\hat{\omega}_{ci}$ is the ion cyclotron frequency in the external magnetic field.

The analysis is carried out within the framework of a hybrid (Vlasov-fluid) model[10] in which the layer electrons and background plasma electrons and ions are described as macroscopic, cold fluids immersed in an axial magnetic field $B_z^0(r)\hat{e}_z$, and the layer ions are described by the Vlasov equation. We assume that the layer is thin, i.e., the radial thickness (2a) of the layer is small in comparison with the mean radius R_0. Equilibrium and stability properties are calculated for the choice of ion layer distribution function in which all the layer ions have the same perpendicular energy in a

frame rotating with angular velocity ω_θ and a step-function distribution in axial velocity v_z [Eq. (2)]. A brief summary of the equilibrium properties and basic assumptions is given in Sec. II. In Sec. III, a hybrid stability analysis is carried out for the case of azimuthally symmetric ($\partial/\partial\theta=0$) perturbations. The purely growing TE mode tearing instability is investigated in Sec. IV, and the necessary and sufficient condition for instability is derived.

Introducing the electrostatic wave admittance $h(kR_0)$ [Eq. (50)], we obtain the critical axial wavenumber for marginal stability ($k=k_c$) from [Eq. (53)],

$$h(k_cR_0)=\nu(R_0^2\omega_\theta^2+\omega_r^2a^2/3)/\Delta^2 ,$$

where ω_r^2 is the radial betatron frequency-squared of the layer ions, and 2Δ is a measure of the total spread on axial velocity. It is found that the system is unstable for perturbations with axial wavenumber k satisfying $0<k<k_c$. Otherwise, the system is stable. Several points are noteworthy in the present analysis. First, a nonzero axial velocity spread ($\Delta\neq0$) stabilizes perturbations with sufficiently short axial wavelength. Second, for specified values of ν and Δ, the unstable range of axial wavenumbers decreases to zero as the conducting wall approaches the ion layer. Finally, the instability growth rate can be reduced to zero by increasing the ratio of plasma density to layer density to arbitrarily large values ($n_p/n_b>>1$).

II. EQUILIBRIUM CONFIGURATION AND BASIC ASSUMPTIONS

As illustrated in Fig. 1, the equilibrium configuration consists of a space-charge neutralized P-layer (proton layer) that is infinite in axial extent and immersed in a cold, dense background plasma. The plasma ions are assumed to be singly charged, and the mean radius and radial thickness of the P-layer are denoted by R_0 and 2a, respectively. A grounded cylindrical conducting wall is located at radius $r=R_c$. Cylindrical polar coordinates (r,θ,z) are introduced. In the present analysis, we make the following simplifying assumptions:

(a) The radial thickness of the P-layer is much smaller than its major radius, i.e.,

$$a \ll R_0 \ . \tag{1}$$

(b) The background plasma electrons (j=e) and ions (j=i), and the layer electrons (j=e') are treated as macroscopic cold fluids ($T_j=0$). In equilibrium, these fluids are assumed to be stationary with zero mean axial motion $[V_{zj}^0(r)=0]$ and zero mean azimuthal motion $[V_{\theta j}^0(r)=\omega_j(r)r=0]$ for j=e,i,e'.

(c) The background plasma equilibrium is assumed to be electrically neutral with $n_i^0(r)=n_e^0(r)$. In addition, the equilibrium charge density of the layer ions (j=b) is neutralized by the layer electrons (j=e') with $n_b^0(r)=n_{e'}^0(r)$. We therefore assume that the equilibrium radial electric field is equal to zero, $E_r^0(r)=0$.

(d) The mean equilibrium motion of the layer ions is in the azimuthal direction, i.e.,

$$\int d^3v \ \underset{\sim}{v} \ f_b^0(\underset{\sim}{x},\underset{\sim}{v})=n_b^0(r)V_{\theta b}^0(r)\hat{\underset{\sim}{e}}_\theta ,$$

where $\hat{e}_{\theta}$ is a unit vector in the θ-direction.

(e) The stability analysis is carried out for azimuthally symmetric ($\partial/\partial\theta = 0$) perturbations.

In the present article, we investigate the equilibrium and stability properties associated with the ion layer distribution function[10]

$$f_b^0(H_\perp-\omega_\theta P_\theta,\ v_z) = \frac{m_i n_b}{4\pi\Delta}\,\delta(U-\hat{T})\Theta[(v_z+\Delta)(\Delta-v_z)]\ , \qquad (2)$$

where n_b, ω_θ, Δ, and $\hat{T}$ are constants, $H_\perp=(m_i/2)(v_r^2+v_\theta^2)$ is the perpendicular energy, $P_\theta=r[m_i v_\theta+(e/c)A_\theta^0(r)]$ is the canonical angular momentum, and the effective energy variable U is defined by

$$U=H_\perp-\omega_\theta P_\theta+m_i R_0^2\omega_\theta^2/2+(e/c)R_0\omega_\theta A_\theta^0(R_0)\ . \qquad (3)$$

In Eq. (2),

$$\Theta(x)=\begin{cases}1\ , & x\geq 0\ ,\\ 0\ , & x<0\ ,\end{cases} \qquad (4)$$

is the Heaviside step function. Here e and m_i are the proton charge and mass, respectively, c is the speed of light in <u>vacuo</u>, and v_r, v_θ, and v_z are the radial, azimuthal, and axial velocities, respectively, of a layer ion. The θ-component of the equilibrium vector potential, $A_\theta^0(r)$, is to be calculated self-consistently from the steady-state $\nabla\times\underset{\sim}{B}_0$ Maxwell equation. Evidently, from Eq. (2), 2Δ is a measure of the total spread in axial velocity.

After some algebraic manipulation, the ion layer density profile for a thin layer is given by[10]

$$n_b^0(r)=\begin{cases}n_b\ , & (r-R_0)^2<a^2\ ,\\ 0\ , & \text{otherwise}\ ,\end{cases} \qquad (5)$$

where the half-thickness of the layer is defined by

$$a=(2\hat{T}/m_i)^{1/2}/\omega_r \ , \tag{6}$$

and

$$\omega_r^2=\omega_{pb}^2\beta_0^2 \ , \tag{7}$$

is the betatron frequency-squared for radial oscillations about the equilibrium radius R_0. In Eq. (7), $\omega_{pb}^2=4\pi e^2 n_b/m_i$ is the plasma frequency-squared for the layer ions, and $\beta_0^2=R_0^2\omega_\theta^2/c^2$. The equilibrium axial magnetic field within the P-layer $[(r-R_0)^2<a^2]$ can be expressed as[10]

$$B_z^0(r)=B_0+(4\pi e/c)n_b\omega_\theta R_0 a[1-(r-R_0)/a] \ , \tag{8}$$

where B_0 is the axial magnetic field outside the layer ($r\geq R_0+a$). For notational convenience in the subsequent analysis, we introduce the effective magnetic compression ratio η defined by

$$\eta=B_z^0(r=R_0-a)/B_0 \ , \tag{9}$$

which characterizes the change in axial magnetic field across the layer. Making use of the definition in Eq. (9), we express Eq. (8) in the equivalent form

$$B_z^0(r) = \frac{B_0}{2}\left[(\eta+1)+(1-\eta)\frac{r-R_0}{a}\right] \ , \tag{10}$$

which is illustrated in Fig. 2.

Defining the ion cyclotron frequency at $r=R_0+a$ by $\hat{\omega}_{ci}=eB_0/m_ic$, it is straightforward to show that[10]

$$\omega_\theta/\hat{\omega}_{ci}=-(1+\eta)/2 \ , \tag{11}$$

which determines the rotation frequency ω_θ in terms of the compression ratio η. We further introduce Budker's parameter for the

layer ions, i.e.,

$$\nu=N_b e^2/m_i c^2=2\pi(e^2/m_i c^2)\int_0^{R_c} dr\ r\ n_b^0(r)\ . \quad (12)$$

Substituting Eq. (5) into Eq. (12) and making use of Eqs. (8), (9), and (11) gives

$$\nu=(1-\eta)/(1+\eta). \quad (13)$$

As illustrated in Fig. 3, we conclude this section by specifying the plasma density profiles by

$$n_j^0(r)=n_p \begin{cases} 1\ , & r<R_0-a\ , \\ [1+\alpha-(1-\alpha)(r-R_0)/a]/2\ , & (r-R_0)^2<a^2\ , \\ \alpha\ , & R_0+a<r<R_c\ , \end{cases} \quad (14)$$

for j=e,i. Here α is an arbitrary constant.

III. STABILITY PROPERTIES FOR AZIMUTHALLY SYMMETRIC PERTURBATIONS

A. Linearized Vlasov-Maxwell Equations

In this section, we make use of the linearized Vlasov-Maxwell equations to investigate stability properties for azimuthally symmetric perturbations ($\partial/\partial\theta=0$) about the thin ion layer equilibrium described by Eq. (2). We adopt a normal-mode approach in which all perturbations are assumed to vary with time t and axial coordinate z according to

$$\delta\psi(\underset{\sim}{x},t)=\hat{\psi}(r)\exp[i(kz-\omega t)],\ \mathrm{Im}\omega>0\ , \tag{15}$$

where ω is the complex eigenfrequency, and k is the axial wavenumber. The Maxwell equations for the TE (transverse electric) mode perturbation can be expressed as

$$\begin{aligned}\hat{B}_r(r)&=-\frac{kc}{\omega}\hat{E}_\theta(r)\ ,\\ \hat{B}_z(r)&=-i\frac{c}{\omega}\frac{1}{r}\frac{\partial}{\partial r}[r\hat{E}_\theta(r)]\ ,\end{aligned} \tag{16}$$

and

$$\left(\frac{\partial}{\partial r}\frac{1}{r}\frac{\partial}{\partial r}r+\frac{\omega^2}{c^2}-k^2\right)\hat{E}_\theta(r)=-\frac{4\pi i\omega}{c^2}\hat{J}_\theta(r). \tag{17}$$

For the TM (transverse magnetic) mode perturbation, we obtain

$$\begin{aligned}\hat{B}_\theta(r)&=\frac{ic}{\omega^2-k^2c^2}\left(\omega\frac{\partial\hat{E}_z(r)}{\partial r}-4\pi k\hat{J}_r(r)\right),\\ \hat{E}_r(r)&=\frac{i}{\omega^2-k^2c^2}\left(kc^2\frac{\partial\hat{E}_z(r)}{\partial r}-4\pi\omega\hat{J}_r(r)\right)\ ,\end{aligned} \tag{18}$$

and

$$\left(\frac{1}{r}\frac{\partial}{\partial r}\, r\, \frac{\partial}{\partial r} + \frac{\omega^2}{c^2} - k^2\right) \hat{E}_z(r) = 4\pi i\left[k\hat{\rho}(r) - \frac{\omega}{c^2}\,\hat{J}_z(r)\right] . \quad (19)$$

In obtaining Eq. (19), use has been made of the continuity equation,

$$-i\omega\hat{\rho}(r) + \frac{1}{r}\frac{\partial}{\partial r}\,[r\hat{J}_r(r)] + ik\hat{J}_z(r) = 0.$$

In Eqs. (16)-(19), $\hat{\underset{\sim}{E}}(r) = \hat{E}_r(r)\hat{\underset{\sim}{e}}_r + \hat{E}_\theta(r)\hat{\underset{\sim}{e}}_\theta + \hat{E}_z(r)\hat{\underset{\sim}{e}}_z$ and $\hat{\underset{\sim}{B}}(r) = \hat{B}_r(r)\hat{\underset{\sim}{e}}_r + \hat{B}_\theta(r)\hat{\underset{\sim}{e}}_\theta + \hat{B}_z(r)\hat{\underset{\sim}{e}}_z$ are the perturbed electric and magnetic fields, and $\hat{\rho}(r)$ and $\hat{\underset{\sim}{J}}(r) = \hat{J}_r(r)\hat{\underset{\sim}{e}}_r + \hat{J}_\theta(r)\hat{\underset{\sim}{e}}_\theta + \hat{J}_z(r)\hat{\underset{\sim}{e}}_z$ are the perturbed charge and current densities. Here $\hat{\underset{\sim}{e}}_r$, $\hat{\underset{\sim}{e}}_\theta$, and $\hat{\underset{\sim}{e}}_z$ are unit vectors in the r, θ, and z-directions, respectively.

As discussed at the beginning of Sec. II, the background plasma components (j=e,i) and layer electrons (j=e') are treated as cold ($T_j \to 0$), macroscopic fluids immersed in an axial magnetic field $B_z^0(r)\hat{\underset{\sim}{e}}_z$. For a thin layer, $B_z^0(r)$ is approximated by

$$B_z^0(r) = B_0 \begin{cases} \eta\,, & 0<r<R_1\,, \\ [(\eta+1)+(1-\eta)(r-R_0)/a]/2, & R_1<r<R_2\,, \\ 1\,, & R_2<r<R_c\,, \end{cases} \quad (20)$$

where $R_1=R_0-a$, and $R_2=R_0+a$ [see Eq. (10)]. The momentum transfer equation and the continuity equation for each cold-fluid component can be expressed as

$$\left(\frac{\partial}{\partial t} + \underset{\sim}{V}_j \cdot \underset{\sim}{\nabla}\right)\underset{\sim}{V}_j = \frac{e_j}{m_j}\left(\underset{\sim}{E} + \frac{\underset{\sim}{V}_j \times \underset{\sim}{B}}{c}\right),$$

$$\frac{\partial}{\partial t}\, n_j + \underset{\sim}{\nabla} \cdot (n_j \underset{\sim}{V}_j) = 0\,, \quad (21)$$

where $n_j(\underset{\sim}{x},t)$ is the density, $\underset{\sim}{V}_j(\underset{\sim}{x},t)$ is the mean fluid velocity, and e_j and m_j are charge and mass, respectively, of a particle of species j.

For azimuthally symmetric perturbations ($\partial/\partial\theta=0$) about a stationary equilibrium, Eq. (21) can be linearized to give

$$
\begin{aligned}
&i\omega\hat{n}_j(r) - \frac{1}{r}\frac{\partial}{\partial r}\left[rn_j^0(r)\hat{V}_{jr}(r)\right]=ikn_j^0(r)\hat{V}_{jz}(r) \ , \\
&i\omega\hat{V}_{jr}(r)+\varepsilon_j\omega_{cj}(r)\hat{V}_{j\theta}(r)= - \frac{e_j}{m_j}\hat{E}_r(r) \ , \\
&i\omega\hat{V}_{j\theta}(r)-\varepsilon_j\omega_{cj}(r)\hat{V}_{jr}(r)= - \frac{e_j}{m_j}\hat{E}_\theta(r) \ , \\
&i\omega\hat{V}_{jz}(r)= - \frac{e_j}{m_j}\hat{E}_z(r) \ ,
\end{aligned}
\tag{22}
$$

where $j=e,i,e'$, and use has been made of $V_{zj}^0(r)=V_{\theta j}^0(r)=0$. In Eq. (22), $\varepsilon_j=\mathrm{sgn}e_j$, $\omega_{cj}(r)=eB_z^0(r)/m_jc$ is the cyclotron frequency, and $\hat{\underset{\sim}{V}}_j(r)$ and $\hat{n}_j(r)$ are the perturbed fluid velocity and density. Denoting the perturbed charge density of the background plasma by $\hat{\rho}_p(r)=e[\hat{n}_i(r)-\hat{n}_e(r)]$, we obtain the approximate relation,

$$
\hat{\rho}_p(r) = \frac{ik}{4\pi}\frac{\omega_{pe}^2(r)}{\omega^2}\hat{E}_z(r) \ , \tag{23}
$$

from the first and last equations of Eq. (22). In obtaining Eq. (23), use has been made of $\omega_{pe}^2 >> \omega_{pi}^2$ and $|\omega|^2 \lesssim \omega_{ci}^2$. Here $\omega_{pe}^2=4\pi e^2n_e^0(r)/m_e$ and $\omega_{pi}^2=4\pi e^2n_i^0(r)/m_i$ denote the plasma frequency-squared of the background electrons and ions, respectively. Substituting Eq. (23) into Eq. (19), we find that Eq. (19) can be approximated in the frequency regime under investigation by

$$
\frac{k^2\omega_{pe}^2(r)}{\omega^2}\hat{E}_z(r)=0 \ , \tag{24}
$$

which gives $\hat{E}_z(r)=0$. We therefore conclude from Eq. (24) that the system is stable for low-frequency TM mode perturbations. In the remainder of this article, we investigate stability properties for TE mode perturbations.

The perturbed azimuthal current density in the regions outside the layer (i.e., $0<r<R_1$ and $R_2<r<R_c$) can be expressed as

$$\hat{J}_\theta(r) = \frac{i}{4\pi} \sum_{j=e,i} \frac{\omega_{pj}^2(r)}{\omega^2-\omega_{cj}^2(r)} \omega\hat{E}_\theta(r) \ . \tag{25}$$

In obtaining Eq. (25), use has been made of Eq. (22) and the TM mode perturbation has been neglected (i.e., $\hat{E}_r=\hat{E}_z=\hat{B}_\theta=0$). Substituting Eq. (25) into Eq. (17), it is straightforward to obtain the eigenvalue equation,

$$\left(\frac{1}{r}\frac{\partial}{\partial r} r \frac{\partial}{\partial r} - \frac{1}{r^2} - p^2\right) \hat{E}_\theta(r)=0 \ , \tag{26}$$

in the regions outside the layer. Here, the effective wavenumber p is defined by

$$p^2= \begin{cases} p_1^2=k^2 + \dfrac{\omega^2\hat{\omega}_{pi}^2}{(\omega^2-\eta^2\hat{\omega}_{ci}^2)c^2} \ , & 0<r<R_1 \ , \\ p_2^2=k^2 + \dfrac{\alpha\omega^2\hat{\omega}_{pi}^2}{(\omega^2-\hat{\omega}_{ci}^2)c^2} \ , & R_2<r<R_c \ , \end{cases} \tag{27}$$

where $\hat{\omega}_{pi}^2=4\pi e^2 n_p/m_i$, $\hat{\omega}_{ci}=eB_0/m_ic$, and αn_p is the plasma density in the region $R_2<r<R_c$. In obtaining Eq. (27), we have defined $\hat{\omega}_{pe}^2 = 4\pi e^2 n_p/m_e$ and $\hat{\omega}_{ce}=eB_0/m_ec$, and use has been made of $\hat{\omega}_{pi}^2/\hat{\omega}_{ci}^2 >> \hat{\omega}_{pe}^2/\hat{\omega}_{ce}^2$ and $|\omega|^2 \lesssim \hat{\omega}_{ci}^2$. The solution to Eq. (26) is given by,

$$\hat{E}_\theta(r)= \begin{cases} AI_1(p_1r) \ , & r<R_1 \ , \\ B\left(I_1(p_2r) - \dfrac{I_1(p_2R_c)}{K_1(p_2R_c)} K_1(p_2r)\right) \ , & R_2<r<R_c \ , \end{cases} \tag{28}$$

where $I_1(x)$ and $K_1(x)$ are modified Bessel functions of the first and second kind, respectively. Defining the normalized wave admittance $b_\pm$ at the inner and outer surfaces of the layer by

$$b_-=[r(\partial/\partial r)\hat{E}_\theta(r)]_{R_1^-}[\hat{E}_\theta(R_1)]^{-1} ,$$
$$b_+=-[r(\partial/\partial r)\hat{E}_\theta(r)]_{R_2^+}[\hat{E}_\theta(R_2)]^{-1} , \tag{29}$$

where $\psi(R_j^\pm)$ denotes $\lim_{\delta\to 0_+}\psi(R_j\pm\delta)$, we obtain

$$b_-=p_1R_1\frac{I_1'(p_1R_1)}{I_1(p_1R_1)} ,$$
$$b_+=p_2R_2\frac{I_1(p_2R_c)K_1'(p_2R_2)-I_1'(p_2R_2)K_1(p_2R_c)}{I_1(p_2R_2)K_1(p_2R_c)-I_1(p_2R_c)K_1(p_2R_2)} , \tag{30}$$

from Eq. (28). Here, the primes (') denote $I_1'(x)=(d/dx)I_1(x)$ and $K_1'(x)=(d/dx)K_1(x)$.

The perturbed azimuthal electric field $\hat{E}_\theta(r)$ is continuous across the layer boundaries (at $r=R_1$ and $r=R_2$). Integrating Eq. (17) from $r=R_1^-$ to $r=R_2^+$, we obtain,

$$R_2\left(\frac{\partial\hat{E}_\theta}{\partial r}\right)_{R_2^+}-R_1\left(\frac{\partial\hat{E}_\theta}{\partial r}\right)_{R_1^-}=\chi(\omega)\hat{E}_\theta(R_0)$$
$$+\int_{R_1}^{R_2}drr\left(\frac{1}{r^2}+k^2-\frac{\omega^2}{c^2}\right)\hat{E}_\theta(r) , \tag{31}$$

where the effective susceptibility is defined by

$$\chi(\omega)\hat{E}_\theta(R_0)=-\frac{4\pi i\omega}{c^2}\int_{R_1^-}^{R_2^+}dr\,r\,\hat{J}_\theta(r) . \tag{32}$$

Making use of Eq. (1), we can neglect the last term on the right-hand side of Eq. (31) for low frequency perturbations with the axial wavenumber satisfying $k^2R_0^2\gtrsim 1$. Substituting Eq. (29) into Eq. (31) gives

$$\chi(\omega)+(b_-+b_+)=0 , \tag{33}$$

where we have approximated $\hat{E}_\theta(r)=\hat{E}_\theta(R_0)$ inside the layer ($R_1<r<R_2$).

Equation (33) is the TE mode dispersion relation for azimuthally symmetric perturbations. Evidently, an evaluation of the effective susceptibility $\chi(\omega)$ is required for a detailed stability analysis.

B. Effective Susceptibility

In this section, we evaluate the perturbed azimuthal current density inside the layer, and the effective susceptibility $\chi(\omega)$ defined in Eq. (32). In determining the azimuthal current density, we approximate the perturbed azimuthal electric field $\hat{E}_\theta(r)$ by,

$$\hat{E}_\theta(r)=\hat{E}_\theta(R_0) \ , \tag{34}$$

for $R_1<r<R_2$. For convenience, we introduce the surface current density σ_j defined by,

$$\sigma_j=\int_{R_1}^{R_2} dr\ \hat{J}_{\theta j}(r) \ , \tag{35}$$

where j=e,i,e',b denotes the plasma electrons and ions, layer electrons, and layer ions, respectively. Making use of Eqs. (10), (14), (22), and (34), it is straightforward to show that the net surface current density carried by the plasma electrons and ions can be expressed as

$$\sigma_p = \frac{i\hat{E}_\theta(R_0)\omega}{8\pi} \sum_{j=e,i} \hat{\omega}_{pj}^2 \int_{R_1}^{R_2} dr\ \frac{1+\alpha-(1-\alpha)\ \dfrac{r-R_0}{a}}{\omega^2-\dfrac{\hat{\omega}_{cj}^2}{4}\left((1+\eta)+(1-\eta)\ \dfrac{r-R_0}{a}\right)^2} \ , \tag{36}$$

where $\hat{\omega}_{pj}^2=4\pi n_p e^2/m_j$ and $\hat{\omega}_{cj}=eB_0/m_j c$ for j=e,i. Carrying out the integration over r in Eq. (36), we obtain

$$\sigma_p = \frac{ia\hat{E}_\theta(R_0)}{4\pi(1-\eta)} \sum_{j=e,i} \frac{\hat{\omega}_{pj}^2}{\hat{\omega}_{cj}^2} \left\{ \hat{\omega}_{cj} \left(1+\alpha+(1-\alpha)\frac{1+\eta}{1-\eta} \right) \right.$$

$$\left. \times \left[\tanh^{-1}\left(\frac{\hat{\omega}_{cj}}{\omega}\right) - \tanh^{-1}\left(\frac{\hat{\omega}_{cj}\eta}{\omega}\right) \right] + \omega \frac{1-\alpha}{1-\eta} \ell n \left(\frac{1-\hat{\omega}_{cj}^2/\omega^2}{1-\hat{\omega}_{cj}^2\eta^2/\omega^2} \right) \right\}, \quad (37)$$

which is valid provided $\mathrm{Im}\omega>0$. [For the special case where $\mathrm{Im}\omega=0$, Eq. (37) can be expressed as a linear combination of $\tanh^{-1}(x)$ and $\coth^{-1}(x)$, thereby avoiding the branch cut on the real ω-axis.] In a similar manner, we find that the layer electron surface current density can be expressed as

$$\sigma_{e'} = \frac{ia\hat{E}_\theta(R_0)}{2\pi(1-\eta)} \frac{\hat{\omega}_{pb}^2}{\hat{\omega}_{ci}} \left[\tanh^{-1}\left(\frac{\hat{\omega}_{ce}}{\omega}\right) - \tanh^{-1}\left(\frac{\hat{\omega}_{ce}\eta}{\omega}\right) \right], \quad (38)$$

where $\hat{\omega}_{pb}^2 = 4\pi e^2 n_b/m_i$. In obtaining Eq. (38), use has been made of the fact that the equilibrium density profile $n_{e'}^0(r)$ for the layer electrons is identical to Eq. (5).

The perturbed distribution function for the layer ions is given by

$$\hat{f}_b(r,\underset{\sim}{p}) = -\frac{e}{m_i} \int_{-\infty}^{0} d\tau \exp\{-i(\omega-kv_z)\tau\} \left(\hat{\underset{\sim}{E}}(r') + \frac{\underset{\sim}{v}'\times\hat{\underset{\sim}{B}}(r')}{c} \right) \cdot \frac{\partial}{\partial \underset{\sim}{v}'} f_b^0 , \quad (39)$$

where use has been made of the axial orbit $z'=z+v_z(t'-t)$. To simplify the right-hand side of Eq. (39), we make use of Eq. (16) and the identity $\partial U/\partial \underset{\sim}{v} = m_i[v_r\hat{\underset{\sim}{e}}_r + (v_\theta - r\omega_\theta)\hat{\underset{\sim}{e}}_\theta]$. Within the context of Eq. (1), it is valid for a thin layer to approximate

$$\theta' = \theta + [\omega_\theta + (v_\perp/R_0)\cos\alpha]\tau , \quad (40)$$

where $v_\perp = [v_r^2 + (v_\theta - \omega_\theta r)^2]^{1/2}$ is the perpendicular speed in a frame of reference rotating with angular velocity ω_θ. Moreover, $v_\perp$ is related to the effective energy variable U by

$$U=(m_i/2)[v_\perp^2+\omega_r^2(r-R_0)^2] ,$$

with $v_\theta-r\omega_\theta=v_\perp\cos\alpha$. After some straightforward algebra, we obtain

$$\hat{f}_b(r,\underset{\sim}{v})=-ie\hat{E}_\theta(R_0)\left(\frac{\partial f_b^0}{\partial U}\, v_\perp\cos\alpha + \frac{k}{m_i\omega}\frac{\partial f_b^0}{\partial v_z}\,(R_0\omega_\theta+v_\perp\cos\alpha)\right)\quad \frac{1}{\omega-kv_z} , \tag{41}$$

where use has been made of Eq. (1), and the fact that the equilibrium distribution function f_b^0 is an even function of v_z and is independent of α. The perturbed azimuthal current density associated with the layer ions is given by

$$\hat{J}_{\theta b}(r)=e\int d^3v\; v_\theta\hat{f}_b(r,\underset{\sim}{v}) . \tag{42}$$

Substituting Eqs. (41) and (42) into Eq. (35) gives

$$\sigma_b=i\,\frac{2ae^2n_b\hat{E}_\theta(R_0)}{m_i\omega}\left(\frac{k^2}{\omega^2-k^2\Delta^2}\,(R_0^2\omega_\theta^2+\frac{1}{3}\,\omega_r^2a^2)+\frac{\omega}{2k\Delta}\,\ell n\left(\frac{\omega+k\Delta}{\omega-k\Delta}\right)\right) \tag{43}$$

for the layer ions.

For notational convenience in the subsequent analysis, we introduce Budker's parameter ν for the layer ions. For a thin layer, we find from Eqs. (5) and (12) that

$$\nu=4\pi R_0an_be^2/m_ic^2=\omega_{pb}^2aR_0/c^2 , \tag{44}$$

where use has been made of Eq. (1). Substituting Eqs. (37), (38), and (43) into Eq. (32), and eliminating n_b in favor of ν, we obtain

$$\chi(\omega)=2\nu\left[k^2\,\frac{R_0^2\omega_\theta^2+\omega_r^2a^2/3}{\omega^2-k^2\Delta^2}+\frac{\omega}{2k\Delta}\,\ell n\left(\frac{\omega+k\Delta}{\omega-k\Delta}\right)\right]$$

$$+\frac{\nu n_p\omega}{(1-\eta)n_b\hat{\omega}_{ci}}\sum_{j=e,i}\left\{\left[(1+\alpha)+(1-\alpha)\,\frac{1+\eta}{1-\eta}\right]\left[\tanh^{-1}\left(\frac{\hat{\omega}_{cj}}{\omega}\right)-\tanh^{-1}\left(\frac{\hat{\omega}_{cj}\eta}{\omega}\right)\right]\right.$$

$$+\frac{\omega(1-\alpha)}{\hat{\omega}_{cj}(1-\eta)}\ln\left(\frac{1-\hat{\omega}_{cj}^2/\omega^2}{1-\hat{\omega}_{cj}^2\eta^2/\omega^2}\right)\Bigg\}+\frac{2\nu\omega}{(1-\eta)\hat{\omega}_{ci}}\left[\tanh^{-1}\left(\frac{\hat{\omega}_{ce}}{\omega}\right)-\tanh^{-1}\left(\frac{\hat{\omega}_{ce}\eta}{\omega}\right)\right], \tag{45}$$

where use has been made of Eq. (1).

Equation (33), when combined with Eqs. (30) and (45), constitutes the final TE mode dispersion relation for azimuthally symmetric perturbations with eigenfrequency satisfying $|\omega| \lesssim \hat{\omega}_{ci}$. Moreover, Eq. (33) can be used to investigate stability properties for a broad range of system parameters.

IV. TEARING MODE INSTABILITY

We now investigate the stability properties predicted by Eq. (33) supplemented by the definitions in Eqs. (30) and (45). The growth rate $\gamma=\mathrm{Im}\omega$ and real oscillation frequency $\Omega_r=\mathrm{Re}\omega$ can be determined from Eq. (33) for a broad range of system parameters ν, Δ, and R_0/R_c, by solving numerically the full transcendental dispersion relation. [Note that the wave admittance $b_\pm$ and the inverse hyperbolic tangent function $\tanh^{-1}(x)$ are generally complicated functions of the complex eigenfrequency ω.] As it is difficult to solve Eq. (33) numerically for general eigenmode, we limit the present analysis to purely growing solutions.

After a careful examination of the effective susceptibility $\chi(\omega)$ in Eq. (45), we note that $\chi(\omega)$ is an even function of the eigenfrequency ω. Moreover, it is evident from Eqs. (27) and (30) that the wave admittances, b_+ and b_-, are also even functions of ω. In this regard, we conclude that there may exist a purely growing solution to Eq. (33) (with $\mathrm{Im}\omega>0$ and $\mathrm{Re}\omega=0$), at least for a certain range of axial wavenumber k. For $-\omega^2=\gamma^2>0$ ($\mathrm{Re}\omega=0$), Eq. (33) can be expressed as

$$\gamma^2 L(k,|\gamma|)=k^2 R(k,|\gamma|) \tag{46}$$

where

$$L(k,|\gamma|)=b_-(P_1R_0)+b_+(P_2R_0)+2\nu\frac{\gamma}{k\Delta}\tan^{-1}\left(\frac{k\Delta}{\gamma}\right)$$

$$+\frac{\nu n_p\gamma}{(1-\eta)n_b\hat{\omega}_{ci}}\sum_{j=e,i}\left\{\left[(1+\alpha)+(1-\alpha)\frac{1+\eta}{1-\eta}\right]\left[\tan^{-1}\left(\frac{\hat{\omega}_{cj}}{\gamma}\right)-\tan^{-1}\left(\frac{\hat{\omega}_{cj}\eta}{\gamma}\right)\right]\right.$$

$$\left.+\frac{\gamma}{\hat{\omega}_{cj}(1-\eta)}\ell n\left(\frac{\gamma^2+\hat{\omega}_{cj}^2\eta^2}{\gamma^2+\hat{\omega}_{cj}^2}\right)\right\}+\frac{2\nu\gamma}{(1-\eta)\hat{\omega}_{ci}}\left[\tan^{-1}\left(\frac{\hat{\omega}_{ce}}{\gamma}\right)-\tan^{-1}\left(\frac{\hat{\omega}_{ce}\eta}{\gamma}\right)\right], \tag{47}$$

and

$$R(k,\gamma^2)=2\nu\left(R_0^2\omega_\theta^2+\omega_r^2\frac{a^2}{3}\right)-L(k,\gamma^2)\Delta^2 \ . \tag{48}$$

In obtaining Eqs. (47) and (48), use has been made of the identity

$$\tanh^{-1}(z) = \frac{1}{2}\,\ell n\left(\frac{1+z}{1-z}\right) = \frac{1}{i}\tan^{-1}(iz) \ .$$

Moreover, p_1 and p_2 are defined by [see Eq. (47)]

$$p_1^2=k^2+\frac{\gamma^2\hat{\omega}_{pi}^2}{(\gamma^2+\eta^2\hat{\omega}_{ci}^2)c^2} \ , \quad p_2^2=k^2+\frac{\alpha\gamma^2\hat{\omega}_{pi}^2}{(\gamma^2+\hat{\omega}_{ci}^2)c^2} \ . \tag{49}$$

For α and η in the range $0 < \alpha < 1$ and $-1 < \eta < 1$, it can be shown from Eq. (47) that $L(k,|\gamma|)$ is positive. Moreover, for appropriate choice of the parameters ν and Δ, the right-hand side of Eq. (46) satisfies $R(k,|\gamma|)\geq 0$ for sufficiently long axial wavelengths, which corresponds to instability.

Defining the total <u>electrostatic</u> wave admittance by [see Eqs. (30) and (49) with $\gamma^2/c^2\to 0$]

$$h(kR_0) = \frac{1}{2}\,kR_0\left[\frac{I_1'(kR_0)}{I_1(kR_0)}+\frac{I_1(kR_c)K_1'(kR_0)-I_1'(kR_0)K_1(kR_c)}{I_1(kR_0)K_1(kR_c)-I_1(kR_c)K_1(kR_0)}\right] , \tag{50}$$

it is readily shown that an upper bound on the growth rate in the unstable region of k-space is given by

$$\gamma^2 \leq k^2\left[\frac{\nu(R_0^2\omega_\theta^2+\omega_r^2a^2/3)}{h(kR_0)}-\Delta^2\right] , \tag{51}$$

because $L(k,|\gamma|) \geq 2h(kR_0)$ follows from Eq. (47). Since $L(k,|\gamma|)$ is positive, it follows from Eq. (46) that the necessary and sufficient condition for instability is given by

$$R(k,|\gamma|) > 0 \ . \tag{52}$$

Moreover, the k-space boundary ($k=k_c$) corresponding to marginal stability ($\gamma=0$) is simply determined from $R(k_c,|\gamma|=0)=0$, which can be expressed as

$$h(k_cR_0)=\nu(R_0^2\omega_\theta^2+\omega_r^2a^2/3)/\Delta^2 \ , \tag{53}$$

where k_c is the critical wavenumber. The system is unstable for perturbations with axial wavenumber in the range $0 < k < k_c$. On the other hand, the system is stable ($\gamma=0$) for short wavelength perturbations with $k>k_c$.

The expression for the electrostatic wave admittance $h(kR_0)$ [Eq. (50)] can be simplified in several limiting cases. These include:

(a) Long wavelength perturbations with $k^2R_0^2 << 1$. In this case, $h(kR_0)$ can be approximated by

$$h(kR_0)=g_f=[1-(R_0/R_c)^2]^{-1} \ . \tag{54}$$

(b) Large conducting wall radius (i.e., $R_c/R_0\to\infty$). In this case

$$h(kR_0) = \frac{1}{2}\,[I_1(kR_0)K_1(kR_0)]^{-1} \ , \tag{55}$$

where use has been made of the identity

$$I_n(z)K_{n+1}(z)+I_{n+1}(z)K_n(z)=1/z \ .$$

(c) Short wavelength perturbations with $k^2R_0^2 >> 1$. In this case, $h(kR_0)$ can be approximated by

$$h(kR_0) = \frac{1}{2}\,kR_0[1+\coth k(R_c-R_0)] \ . \tag{56}$$

The function $h(kR_0)$ is plotted versus kR_0 for various values of R_0/R_c in Fig. 4. Note that $h(kR_0)$ is a monotonic increasing function

of kR_0. For appropriate choice of the parameters ν and Δ, and a specified value of R_0/R_c it is clear that the constant function $\nu(R_0^2\omega_\theta^2+\omega_r^2a^2/3)/\Delta^2$ will intersect the curve $h(kR_0)$ at some critical k-value ($k=k_c$), and the system will be unstable for $0 < k < k_c$. On the other hand, if Budker's parameter ν and axial velocity spread Δ satisfy the inequality

$$\nu(R_0^2\omega_\theta^2 + \frac{1}{3}\omega_r^2a^2)/\Delta^2 < g_f \ , \tag{57}$$

the system is stable over the entire region of k-space. That is, Eq. (57) is a necessary and sufficient condition for stability. Making use of $\omega_r^2=\omega_{pb}^2\beta_0^2=\omega_{pb}^2R_0^2\omega_\theta^2/c^2$ [Eq. (7)], $\omega_{pb}^2a^2/c^2=\nu a/R_0$ [Eq. (44)], and $\omega_\theta/\hat{\omega}_{ci}=-(1+\nu)^{-1}$ [Eq. (11)], the necessary and sufficient condition for stability [Eq. (57)] can be expressed as

$$\frac{\Delta^2}{R_0^2\hat{\omega}_{ci}^2} > [1-(R_0/R_c)^2]\,\frac{\nu}{(1+\nu)^2}\left(1+\frac{\nu}{3}\frac{a}{R_0}\right) \ , \tag{58}$$

or equivalently,

$$\frac{\Delta^2}{R_0^2\hat{\omega}_{ci}^2} > \frac{1}{4}\,[1-(R_0/R_c)^2]\left((1-\eta^2)+\frac{1}{3}\frac{a}{R_0}(1-\eta)^2\right) \ , \tag{59}$$

where use has been made of $\nu=(1-\eta)/(1+\eta)$ [Eq. (13)].

Several points are noteworthy from Eqs. (53) and (58) and Fig. 4. First, a nonzero axial velocity spread ($\Delta\neq0$) tends to stabilize perturbations with sufficiently short axial wavelength [Eq. (53)]. Indeed, for sufficiently large Δ, the tearing mode instability can be completely stabilized [Eq. (58)]. If the layer density is sufficiently low that $\nu << 1$, then the critical value of Δ required for stabilization is $\Delta_{cr}/R_0\hat{\omega}_{ci}=[1-(R_0/R_c)^2]^{1/2}\nu^{1/2}$. On the other hand, for a high-density layer with $\nu >> 1$, Eq. (58) gives $\Delta_{cr}/R_0\hat{\omega}_{ci}=[1-(R_0/R_c)^2]^{1/2}(a/3R_0)^{1/2}$, which is generally more difficult to

satisfy. A second important feature of the instability is the fact that the presence of a conducting wall has a stabilizing influence. Indeed, as $(R_c-R_0)/R_c=\varepsilon\to 0$, the critical value of Δ required for stabilization scales as $\varepsilon^{1/2}$ [Eq. (58)]. Finally, we note from Eqs. (53) and (58) that the range of unstable k-values and the necessary and sufficient condition for stability are independent of background plasma properties (i.e., independent of plasma density n_p). However, the value of the growth rate γ obtained from Eq. (46) does depend sensitively on n_p through the definition of $L(k,|\gamma|)$ in Eq. (47).

In order to illustrate the dependence of growth rate γ on the density ratio n_p/n_b, we Taylor-expand $L(k,|\gamma|)$ about $\gamma=0$ and retain terms of order γ. Making use of the approximation $\tan^{-1}(1/x) \simeq (\pi/2)\mathrm{sgn}x$ for $x\ll 1$, it is straightforward to show that

$$L(k,|\gamma|) = 2h(kR_0) + 2\nu\,\varepsilon(\eta)|Z| \quad , \tag{60}$$

where the function $\varepsilon(\eta)$ is defined by

$$\frac{2}{\pi}\,\varepsilon(\eta) = \frac{\hat{\omega}_{ci}}{k\Delta} + \left\{ \frac{n_p}{n_b}\left[(1+\alpha) + (1-\alpha)\,\frac{1+\eta}{1-\eta}\right] + 1 \right\} \frac{1-\mathrm{sgn}\eta}{1-\eta} \tag{61}$$

and $Z = \gamma/\hat{\omega}_{ci}$ is the normalized growth rate. Substitution of Eq. (61) into Eqs. (46) and (48) gives a cubic equation for Z which is valid when $|Z| \ll 1$. For a field-reversed layer ($\eta<0$) in a dense background plasma satisfying $n_p \gg n_b$, Eq. (61) can be further simplified to give

$$\varepsilon(\eta) = \frac{n_p}{n_b}\left[(1+\alpha) + (1-\alpha)\,\frac{1+\eta}{1-\eta}\right]\frac{\pi/2}{1-\eta} \quad . \tag{62}$$

In the case where the density ratio n_p/n_b is sufficiently large that

$(n_p/n_b)|Z| >> h(kR_0)$, the dispersion relation in Eq. (46) can be approximated by

$$Z^2|Z|\varepsilon(\eta) = [kR_0/(1+\nu)]^2 \tag{63}$$

where use has been made of $a/R_0 << 1$, and the assumption $(\Delta/R_0\hat{\omega}_{ci})<<1$. In Eq. (63), $\varepsilon(\eta)$ is defined in Eq. (62). It is obvious from Eq. (63) that the instability growth rate is given by

$$\frac{\gamma}{\hat{\omega}_{ci}} = \left[\frac{2n_b/\pi n_p}{(1-\eta)(1+\alpha)+(1+\eta)(1-\alpha)}\right]^{1/3}\left[\frac{kR_0(1-\eta^2)}{2}\right]^{2/3} \tag{64}$$

Evidently, from Eq. (64), the growth rate γ decreases with increasing n_p/n_b, and can be significantly reduced in the limit of large background plasma density with $n_p/n_b>>1$.

Finally, we conclude this section by pointing out two areas in which the present analysis can be generalized. First, the analysis can be extended to investigate stability behavior for non-zero real eigenfrequency. Second, the present analysis can be extended in a relatively straightforward manner to circumstances where the perturbations are not azimuthally symmetric ($\partial/\partial\theta\neq 0$). In this case, the tearing mode instability will couple with the negative-mass instability[10] and the corresponding analysis will be more complicated.

V. CONCLUSIONS

In this paper, we have examined the tearing-mode stability properties of an intense field reversed P-layer immersed in a background plasma. The analysis was carried out within the framework of a hybrid Vlasov-fluid model. The equilibrium properties (Sec. II) and stability properties (Secs. III and IV) for azimuthally symmetric perturbationshave been investigated for the choice of ion layer distribution function in which all ions have the same perpendicular energy in a frame rotating with angular velocity ω_θ and a step-function distribution in axial velocity v_z. A detailed analytic and numerical investigation of stability properties was carried out in Sec. IV for the purely growing tearing mode. The most important conclusions drawn from this study are the following. First, an axial velocity spread ($\Delta \neq 0$) has a stabilizing influence for perturbations with sufficiently short axial wavelength. Second, for specified values of ν and Δ, the range of axial wave-number corresponding to instability decreases to zero as the conducting wall radius approaches the radius of the ion layer. Finally, the instability growth rate can be reduced to zero provided the ratio of plasma density to beam density is sufficiently large.

ACKNOWLEDGMENTS

This research was supported by the Office of Naval Research under the auspices of a joint program with the Naval Research Laboratory. The research by one of the authors (H.S.U.) was supported in part by the electron beam propagation project in the Naval Surface Weapons Center. It is a pleasure to acknowledge the benefit of useful discussions with Dr. Jim Drake.

REFERENCES

1. H. A. Davis, R. A. Meger, and H. H. Fleischmann, Phys. Rev. Lett. 37, 542 (1976).
2. C. A. Kapetanakos, J. Golden, and K. R. Chu, Plasma Phys. 19, 387 (1977).
3. A. Mohri, K. Narihara, T. Tsuzuki, and Y. Kubota, in Proceedings 2nd International Topical Conference on High Power Electron and Ion Beam Research and Technology (Ithaca, N. Y. 1977), Vol. I, p. 459.
4. D. E. Baldwin and M. E. Rensink, Comments on Plasma Physics and Controlled Fusion, in press (1978).
5. K. D. Marx, Phys. Fluids 11, 357 (1968).
6. R. V. Lovelace, Phys. Rev. Lett. 35, 162 (1975).
7. R. N. Sudan and M. N. Rosenbluth, Phys. Rev. Lett. 36, 972 (1976).
8. J. M. Finn and R. N. Sudan, Phys. Rev. Lett. 41, 695 (1978).
9. H. S. Uhm and R. C. Davidson, Phys. Fluids, in press (1979).
10. H. S. Uhm and R. C. Davidson. Phys. Fluids, in press (1979).
11. J. F. Drake and Y. C. Lee, Phys. Fluids 20, 1341 (1977).

FIGURE CAPTIONS

Fig. 1 Equilibrium configuration and coordinate system.

Fig. 2 Equilibrium magnetic field profile [Eq. (10)].

Fig. 3 Electron and ion density profiles for the background plasma [Eq. (14)].

Fig. 4 Plot of electrostatic wave admittance $h(kR_0)$ [Eq. (50)] versus normalized axial wavenumber kR_0 for several values of the parameter R_0/R_c. The dashed line represents $h(k_cR_0)=\nu(R_0^2\omega_\theta^2+\omega_r^2a^2/3)/\Delta^2=3$ [Eq. (53)].

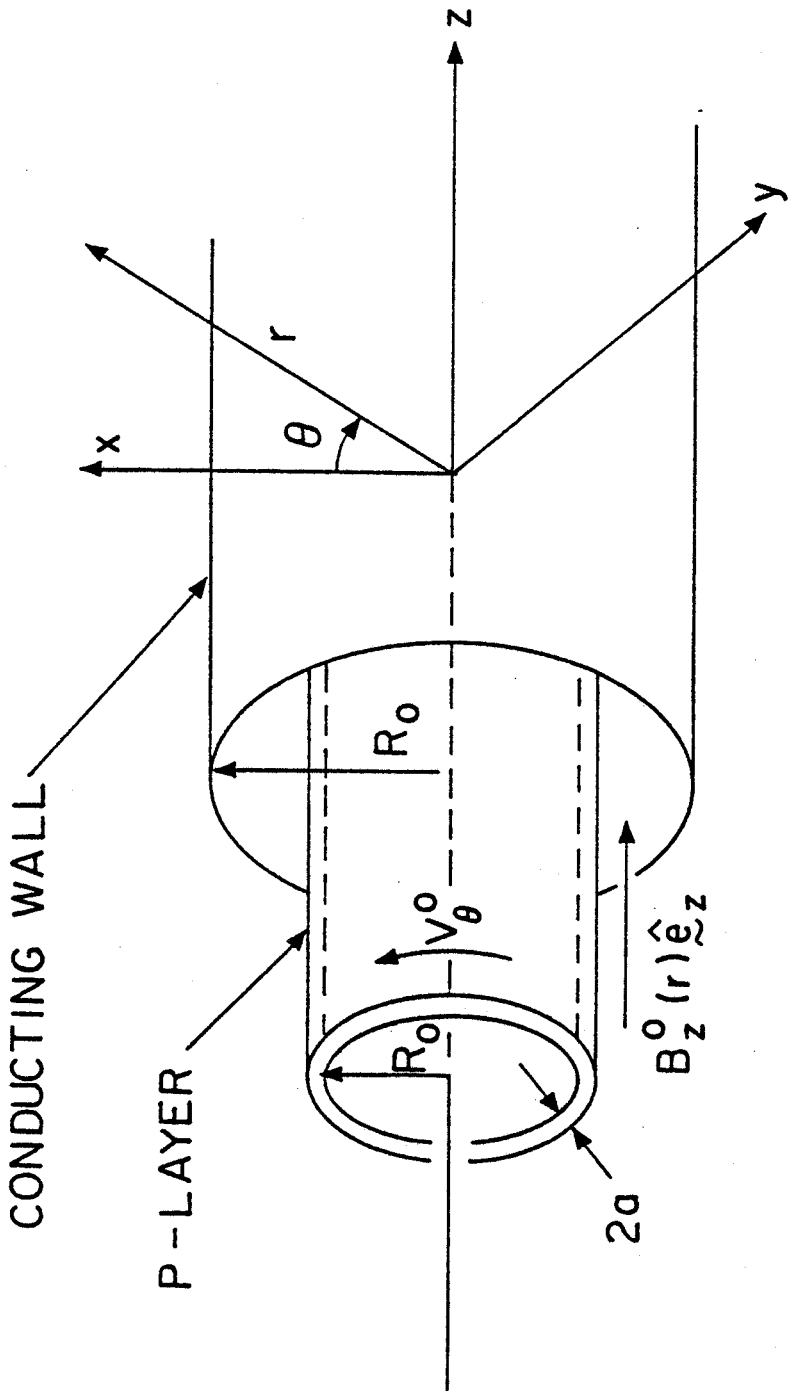

Fig. 1

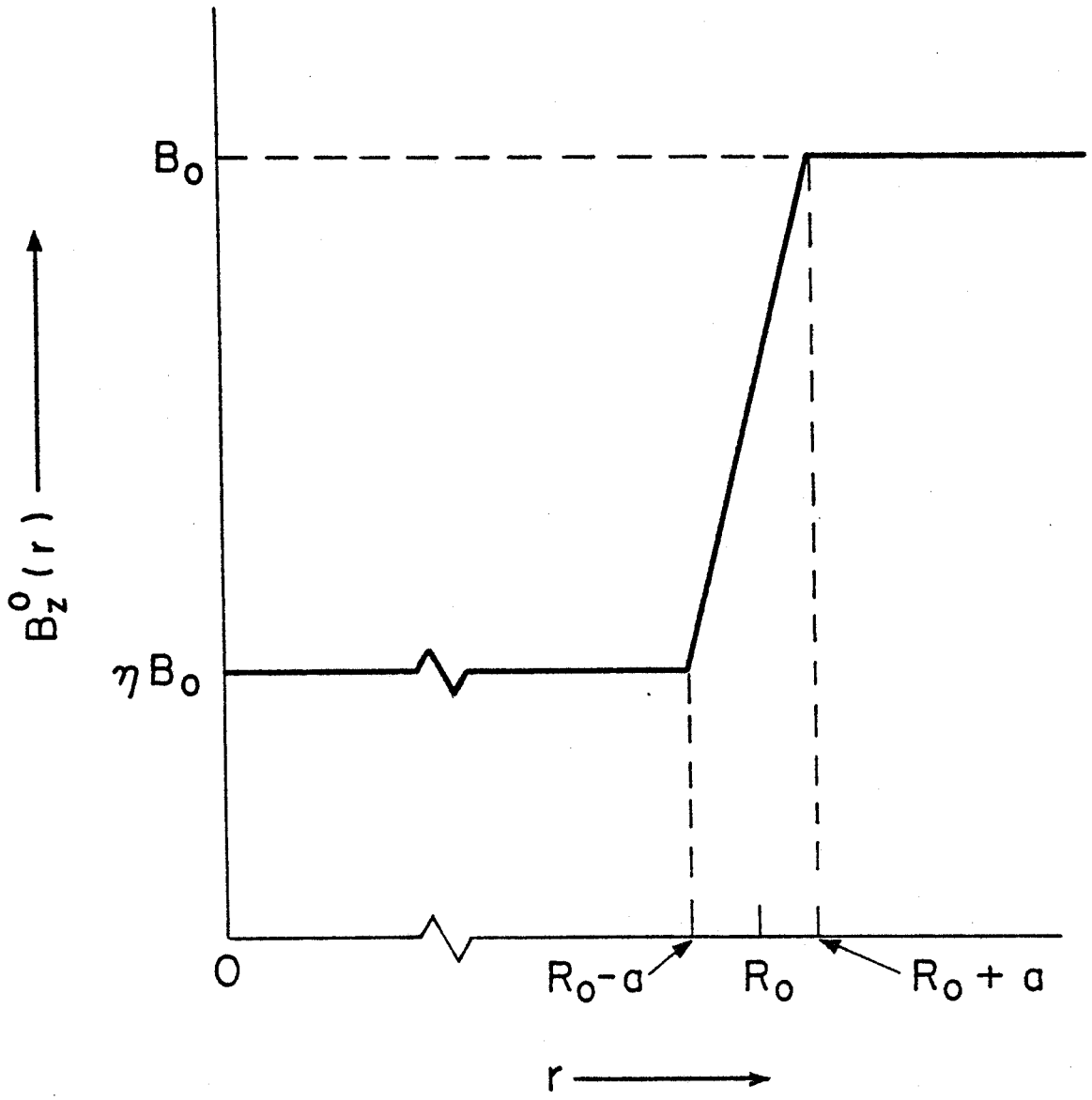

Fig. 2

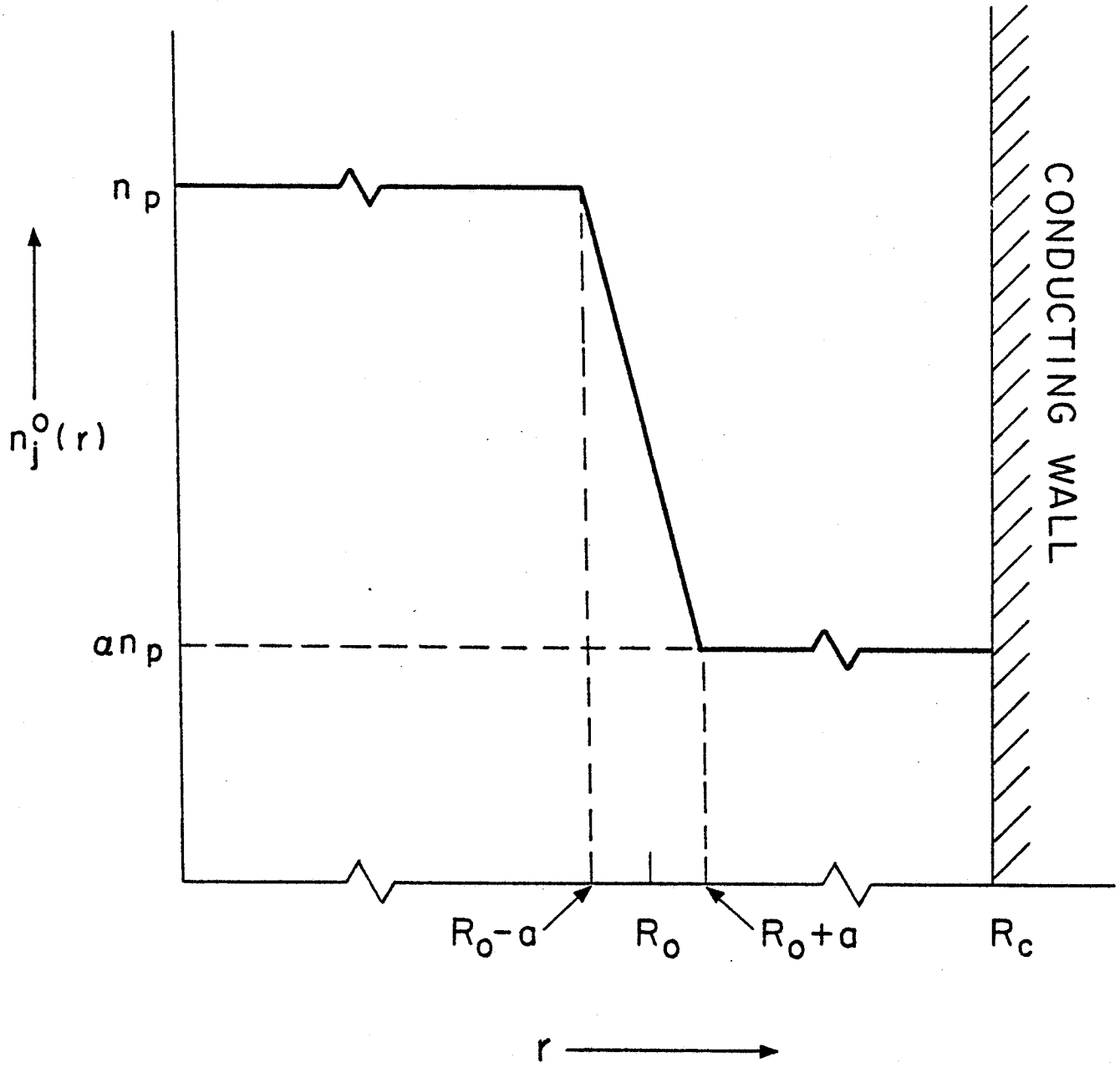

Fig. 3

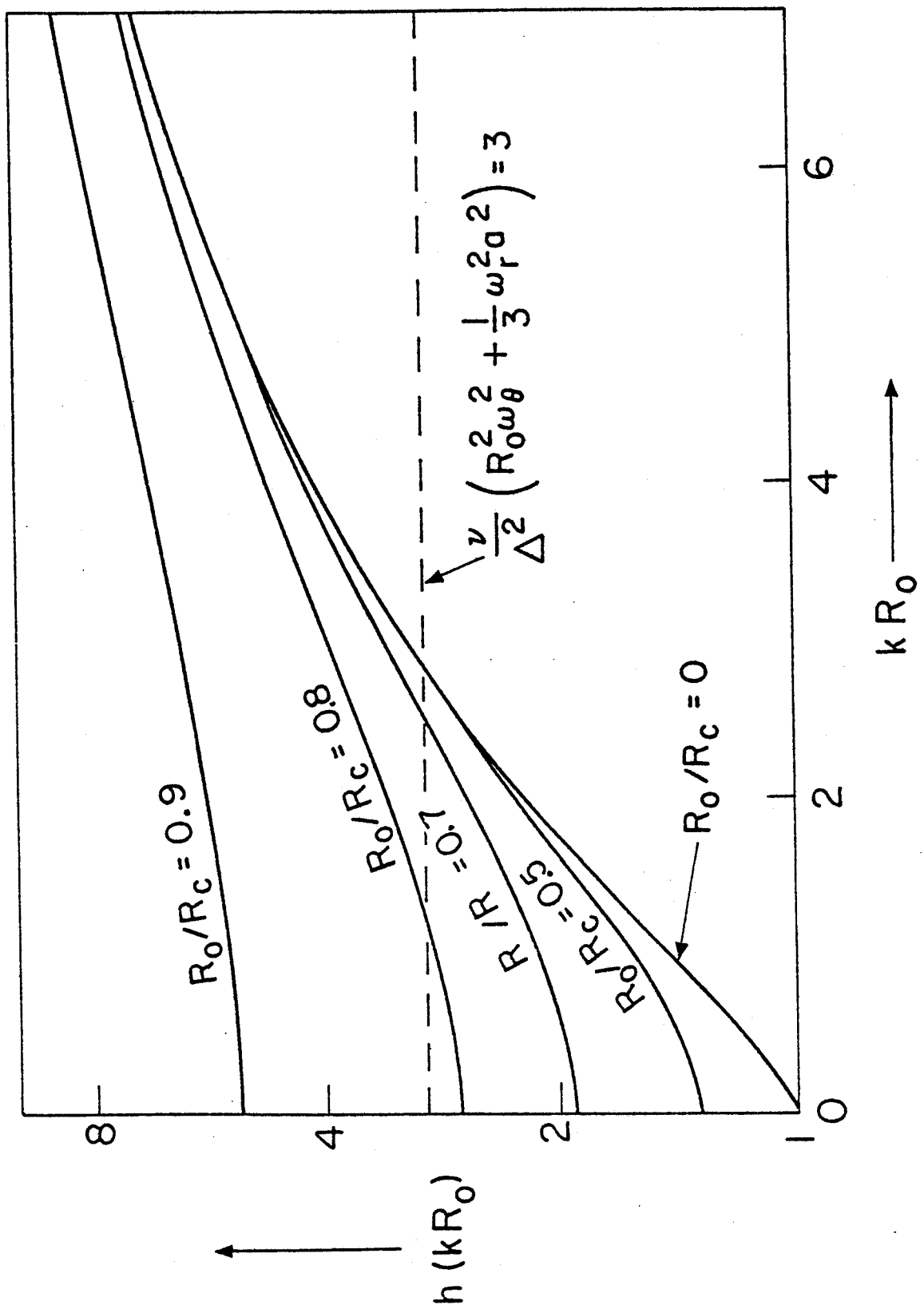
h (kR_o)
kR_o
R_o/R_c = 0.9
R_o/R_c = 0.8
R_o/R_c = 0.7
R_o/R_c = 0.5
R_o/R_c = 0
ν/Δ² (R_o²ω_θ² + 1/3 ω_r²a²) = 3
8
4
2
1
0
2
4
6

Fig. 4